

# Wannier exciton states in a 1D topological chain

**Author:**

Zhiwei Wang  
Master student Theoretical Physics,  
Utrecht University

**First supervisor:**

Prof. Dr. Ir. H.T.C. Stoof  
Institute for Theoretical Physics and  
Center for Extreme Matter and Emergent Phenomena,  
Utrecht University

**Second supervisor:**

Dr. L. Fritz  
Institute for Theoretical Physics and  
Center for Extreme Matter and Emergent Phenomena,  
Utrecht University

Master Thesis



**Universiteit Utrecht**

Institute for Theoretical Physics  
Utrecht University  
September, 07, 2021

## Abstract

This thesis investigates the properties of 1D Wannier excitons in a 1D s-p wave hybrid chain. Based on the tight-binding model, we first calculate the winding number of the single-electron band structure. Then, we introduce the particle-hole basis with the interband Coulomb interaction in 1D to determine the bound-state spectrum and the dispersion relation of excitons. Finally, we calculate the winding number for the exciton states themselves and show that it is exactly twice as large as the single-electron winding number in the same 1D chain.

## Contents

<b>1</b>	<b>Introduction to topological exciton</b>	<b>2</b>
1.1	Motivation . . . . .	2
1.1.1	Why topological? . . . . .	2
1.1.2	Why excitons? . . . . .	2
1.1.3	Interplay between topological insulators and excitons . . . . .	3
1.1.4	What did we do? . . . . .	3
1.2	Outline . . . . .	3
1.3	Conventions . . . . .	3
<b>2</b>	<b>1D s-p hybridization chain lattice model</b>	<b>4</b>
2.1	Hamiltonian . . . . .	4
2.2	Eigenstates . . . . .	5
2.3	Topological Invariant . . . . .	7
<b>3</b>	<b>Excitons with bare Coulomb interaction</b>	<b>7</b>
3.1	The physical picture . . . . .	7
3.2	Hydrogen-like eigenenergies . . . . .	9
<b>4</b>	<b>Coulomb matrix elements in 1D chain</b>	<b>10</b>
4.1	Hamiltonian . . . . .	10
4.2	Matrix elements in real space . . . . .	11
4.3	Matrix elements in momentum space . . . . .	15
<b>5</b>	<b>Microscopic derivation of excitons</b>	<b>16</b>
5.1	Electron-hole basis . . . . .	16
5.2	Non-interacting part . . . . .	16
5.3	Interacting part . . . . .	16
5.4	Eigenstates . . . . .	17
<b>6</b>	<b>Eigenenergies and dispersion relation</b>	<b>18</b>
6.1	Numerical method to solve the Schrödinger equation . . . . .	18
6.2	Numerical solution of the exciton eigenenergies in effective mass approximation . . . . .	19
6.3	Numerical solution of the exciton dispersion relation with full band structure . . . . .	21
<b>7</b>	<b>Topological properties of excitons</b>	<b>22</b>
<b>8</b>	<b>Conclusion</b>	<b>23</b>

# 1 Introduction to topological exciton

## 1.1 Motivation

We ask ourselves two questions: what is the effect of the electronic topology on the exciton properties and why we study such a system?

### 1.1.1 Why topological?

At an early age, solid-state physics [1] [2] classified all the band insulators (including semiconductors at the low temperature) to be the same phase because the energy gap between valance and conduction band is tunable continuously. However, the discovery of the integer quantum Hall effect (1980) [3] has shown that, under a strong magnetic field, the finite-size 2D electron gas is not just an insulator in the bulk due to the Landau localization [4] but also can transport electrons by bouncing them off the boundary. This means that not all band insulators can be classified into the same phase. Two years after the experiment, Thouless, Kohmoto, Nightingale and den Nijs (TKNN) [5] used the Kubo formula [6] to calculate the Hall conductivity and relate it with the topology of the band structure. Their work opened a new window to classify materials by their topology. These phases are distinguished by a topological invariant called the TKNN invariant or the Chern invariant.

After the integer quantum Hall effect, the idea of the topological phase was booming and was extended [7] [8] [9] beyond the free electron gas. Kane and Mele [10] proposed a quantum Hall effect model in graphene where no external magnetic field was needed. Graphene is a monolayer Graphite that has a special dispersion relation near the Dirac point. By introducing the spin-orbital interaction instead of external magnetic field, the energy gap can be lifted without breaking time-reversal symmetry [9]. As a result, the spin Hall effect has been predicted and achieved by Hall currents that flow in opposite directions without an external magnetic field [9].

This topological phase can also be introduced into a 3D system which generalizes the edge state to surface state. In a 2D system, the Hall conductivity is always an integer in the unit of  $\frac{e^2}{h}$  [7] due to the fermion doubling theorem [11], while this theorem is no longer valid in 3D [7]. When a gap is opened on the surface, a single Dirac fermion exhibits a half-integer Hall conductance due to chiral symmetry breaking when the magnetic field [12] [13] is applied. Theoretically, it means that a mass term makes the original (massless) fermion massive. Proposed by Seradjeh, Moore, and Franz in 2009 [14], this mass term can also be introduced by the Coulomb interaction between the electron and hole pair.

From an application perspective, topological insulators are novel quantum materials for electronic devices due to their unusual properties [15]. For example, in  $Bi_2Se_3$  and  $Bi_2Te_3$ , the backscattering is suppressed in the edge state and immune to various structural defects and imperfections as long as time-reversal symmetry is preserved. This makes topological insulators highly promising to be used in energy-efficient devices. Furthermore, strong spin-orbit coupling in these materials leads to the spin-momentum locking effect, namely, the spin is “locked” relative to the momentum. This property means that the spins are polarized automatically, making these materials highly suitable for spintronic devices. Another potential application is Majorana-based quantum computation [7] since it can store qubits nonlocally and thus becomes robust against noise.

### 1.1.2 Why excitons?

Firstly, excitons play a vital role in explaining the interband transition spectra in a semiconductor [16]. As pointed out by Wannier [17], when a semiconductor absorbs a photon, it will create an electron-hole pair which is a two-particle process [18]. Then this electron-hole pair can form a hydron-like quasiparticle by the Coulomb interaction, and thus it influences absorption and luminescence spectra of the semiconductor [16] [19].

Secondly, the exciton system serves as a good candidate to study many-body effects since it is well-coupled with photons [20] and suitable for experimental manipulation. Many-body effects [21] are important when a single noninteracting electron basis framework is inadequate. In the early era, pioneers like Paul Drude and Arnold Sommerfeld studied metal conductivity and heat capacity by the free electron gas model [2]. However, such an oversimplified non-interacting electron-gas model failed when more experiments results popped up. For instance, conventional superconductivity - condensation of fermionic pairs - is a many-body effect where the fermions are attracted to each other and the interaction is mediated by phonons [22]. This stunning example urges us to include

the many-body effect in our simplified model of a single-electron state in the non-interacting framework.

Thirdly, exciton superfluidity has the potential to reach the high  $T_c$  [23]. Excitons are formed by electron-hole pairs and thus can be viewed as composite bosons [20]. As composite bosons [20], they can undergo Bose-Einstein condensation (BEC). Due to the smaller effective mass, excitons are predicted to condense at considerable high temperatures [23].

From an engineering application like light-emitting diode, bound excitons play a vital role in semiconductor luminescence. In indirect band semiconductor materials, due to the limitation of the momentum selection rule, the material's luminescence is usually very weak. But if there are bound excitons, whose wavefunction is localized in space, the above momentum selection rule of the luminescence transition can be remarkably relaxed, and there is a great probability of luminescence transition without the participation of phonons. Through this process, the luminous efficiency of the indirect band material will be greatly enhanced [24].

### 1.1.3 Interplay between topological insulators and excitons

The exciton system offers us a new platform to play with topological insulators beyond original electronic systems. Usually, people are interested in topological insulators because of their unique boundary states and lack of discussion of bulk properties. For instance, two thin layers of topological insulators with opposite carriers can form into the topological excitonic condensate (TEC) [25], a coherent many-body state. The TEC is electronic superfluid and supports dissipationless neutral charge transport, which can empower ultralow-power transistors [15]. However, the bulk excitons are crucial to explaining the photoexcitation-related process in different systems like light-emitted dioxide, laser, and solar cells. This urges us to also investigate the bulk property of excitons, especially in the case of nontrivial topological materials like 2D monolayer transition metal dichalcogenides. We can talk much more about why the interplay between topological insulators and excitons is charming, like the optical selection rule due to the freedom of valley exciton [26] or the half quantum integer effect caused by exciton in 3D [7]; nevertheless, we restrict ourselves for the time being.

### 1.1.4 What did we do?

We choose to investigate the dispersion relation and topological invariant of a toy model: A Wannier exciton state in a 1D s-p wave hybrid topological chain with correct long-range Coulomb interaction. We choose the 1D chain because it is the minimal model which captures the vital topological properties, while one exciton (two-particle pair) serves as the minimal many-body effect.

## 1.2 Outline

In section 2, we begin with a 1D s-p wave hybrid chain by writing down the Hamiltonian without Coulomb interaction. Under the framework of noninteracting electrons, the winding number of the band structure has been calculated under different choices of on-site hybridization and hopping terms.

In section 3, we phenomenologically introduce the model of excitons and show that it has a hydrogen-like nature.

In section 4, we explicitly calculate the Coulomb matrix element in the 1D chain, which is useful in later computations.

In section 5, we derive the Hamiltonian of excitons microscopically by adding Coulomb interaction terms into the band Hamiltonian and particle-hole operators.

In section 6, we first calculate the eigenenergies and eigenstates of exciton with zero total momentum  $Q$ . Then we calculate the dispersion relation of exciton by turning on the total momentum  $Q$ .

In section 7, we calculate the winding number of the wavefunction of the exciton which turns out to be exactly bigger as much as that of the electron.

In section 8, we make a conclusion.

## 1.3 Conventions

1.  $\stackrel{Mma}{=}$  means that we run the calculation in the software Mathematica.
2. Both letter P and Q are used as total momentum of the systems.
3. We use natural units in our thesis to simply the calculation, namely set  $\hbar = m = e = 1$ . Still, we sometimes keep the units for readability.

4. Letter "m" represents the mass of a free electron, while  $m_e$  and  $m_h$  represent the effective mass of electron and hole.
5. We represent the lattice constant as letter "a".
6. We choose the Bohr radius  $a_0$  as the length scale for interatomic Coulomb matrix element in chapter 4. We can use the relation  $\rho=c R=\frac{R}{a_0}$  to convert the distance between nuclei into a dimensionless quantity. Be careful, the distance between nuclei  $R$  in chapter 4 is different to lattice constant  $a$ .
7. We rescale the length unit of the Coulomb matrix element when we introduce the Coulomb into the band Hamiltonian. As a result,  $\tilde{\rho}=\frac{R}{a}=\frac{R}{a_0}\frac{a_0}{a}=\rho\frac{a_0}{a}$  and  $\tilde{k}=\frac{a}{a_0}k$ .
8. We use letter "a" as creation and annihilation operator, while we use letter "c" to represent the s wave and letter "p" for the p wave respectively.
9. The typical energy scale of the gap is eV (same as on-site terms and hopping terms), which is around 10 times smaller than the ground state of hydrogen atom.
10. The typical energy scale of the exciton is 1000 times smaller than the Rydberg constant in 3D because of the smaller effective mass and large dielectric constant.
11. The typical energy scale of the exciton is 10 times smaller than the Rydberg constant in 1D because the dielectric constant is almost 1 in 1D.
12. The typical effective mass of an electron or a hole is one order of magnitude less massive than a free electron.

## 2 1D s-p hybridization chain lattice model

In this section, we first use the tight-binding method to describe the band structure of 1D chain with the s and p wave orbitals, which are eigenfunctions of a single isolated atom. The band structure describes the single-electron state of the system, assuming no interaction with lattice vibrations. Further, we Fourier transform the Hamiltonian into momentum space to get the eigenstates and eigenenergies of the system.

### 2.1 Hamiltonian

The tight-binding model [1] is a method to calculate the electronic band structure using a set of localized atomic wavefunctions. The starting point of the tight-binding approximation is that when an electron is near an atom, it will mainly feel the effect of the atomic field, and the effect of other atomic fields can be regarded as a perturbation effect. From this model, we can get the one-electron eigenstates— Bloch states — which can be used as the basis for calculating the winding number and to form the basis of electron-hole Wannier exciton problem. We begin with the lattice Hamiltonian

$$\begin{aligned}\hat{H} &= \hat{H}_0 + \hat{H}_{int} \\ &= \int dx \Psi^+(x) \left\{ -\frac{\hbar^2 \nabla^2}{2m} + V^{ex}(x) \right\} \Psi(x) + \frac{1}{2} \int dx \int dx' \Psi^+(x) \Psi^+(x') V(x-x') \Psi(x') \Psi(x),\end{aligned}\quad (2.1)$$

where the external potential is described by

$$V^{ex}(x) = V^{ion}(x) = V^{ion}(x + mR_0),\quad (2.2)$$

with  $R_0$  as the distance between two atomic nuclei. Using the Wannier functions, we can expand the field operator [27] in a basis as

$$\Psi(x) = \sum_{n,i} a_{i,n} w_n(x - x_i).\quad (2.3)$$

Here we consider a 1D chain lattice model with only s wavefunctions and p wavefunctions as shown in Figure 1. Meanwhile, only the  $\sigma$  bond part of  $p-p$  interaction, namely the interaction along the direction of chain will be considered. We keep these two terms because they are the two main terms describing the low-energy excitations, which are the essential terms for the Wannier excitons.

For the non-interacting part, we can get

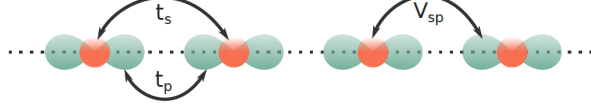


Figure 1: 1D chain model with s and p wave hopping terms [28].

$$\begin{aligned}
H_0 = \sum_j \left\{ \epsilon_s c_j^\dagger c_j + \epsilon_p p_j^\dagger p_j \right. \\
- t_{s,s;j,j+1} c_j^\dagger c_{j+1} - t_{s,s;j+1,j} c_{j+1}^\dagger c_j - t_{p,p;j,j+1} p_j^\dagger p_{j+1} - t_{s,s;j+1,j} p_{j+1}^\dagger p_j \\
\left. - t_{s,p;j,j+1} c_j^\dagger p_{j+1} - t_{s,p;j+1,j} c_{j+1}^\dagger p_j - t_{p,s;j,j+1} p_j^\dagger c_{j+1} - t_{p,s;j+1,j} p_{j+1}^\dagger c_j \right\},
\end{aligned} \tag{2.4}$$

where

$$t_{n,m;i,j} = - \int dx w_n^*(x - x_i) \left( -\frac{\hbar^2 \nabla^2}{2m} + V^{ex}(x) \right) w_m(x - x_j). \tag{2.5}$$

Due to the symmetry of s and p wave function, we can simplify the hopping terms as

$$t_s = +t_{s,s;j,j+1} = +t_{s,s;j+1,j}, \tag{2.6}$$

$$t_p = -t_{p,p;j,j+1} = -t_{p,p;j+1,j}, \tag{2.7}$$

$$V_{sp} = -t_{s,p;j,j+1} = +t_{s,p;j+1,j} = -t_{p,s;j,j+1} = +t_{p,s;j+1,j}. \tag{2.8}$$

Using these definitions, Eq. 2.4 becomes,

$$\begin{aligned}
H_0 = \sum_j \left\{ \epsilon_s c_j^\dagger c_j + \epsilon_p p_j^\dagger p_j \right. \\
- t_s (c_j^\dagger c_{j+1} + c_{j+1}^\dagger c_j) + t_p (p_j^\dagger p_{j+1} + p_{j+1}^\dagger p_j) \\
\left. + V_{sp} (c_j^\dagger p_{j+1} - c_{j+1}^\dagger p_j) - V_{sp} (p_j^\dagger c_{j+1} - p_{j+1}^\dagger c_j) \right\}.
\end{aligned} \tag{2.9}$$

## 2.2 Eignstates

In order to get the eignstates of such a lattice model, we can Fourier transform the Hamiltonian into momentum (crystal momentum) space by

$$\begin{aligned}
c_j^\dagger = \frac{1}{\sqrt{L}} \sum_k e^{-ikr_j} c_k^\dagger, c_j = \frac{1}{\sqrt{L}} \sum_k e^{+ikr_j} c_k, \\
p_j^\dagger = \frac{1}{\sqrt{L}} \sum_k e^{-ikr_j} p_k^\dagger, p_j = \frac{1}{\sqrt{L}} \sum_k e^{+ikr_j} p_k.
\end{aligned} \tag{2.10}$$

We can get the Hamiltonian in momentum space

$$H_0 = \sum_k H_0(k) = \sum_k \begin{pmatrix} c_k^\dagger & p_k^\dagger \end{pmatrix} \begin{pmatrix} \epsilon_s - 2t_s \cos(ka) & 2iV_{sp} \sin(ka) \\ -2iV_{sp} \sin(ka) & \epsilon_p + 2t_p \cos(ka) \end{pmatrix} \begin{pmatrix} c_k \\ p_k \end{pmatrix}, \tag{2.11}$$

where letter "a" is the distance between the nearest ions. We can write  $H_0$  succinctly as

$$H_0(k) = \begin{pmatrix} d_0(k) + d_z(k) & -id_y(k) \\ +id_y(k) & d_0(k) - d_z(k) \end{pmatrix}, \tag{2.12}$$

$$H_0(k) = d_0(k)I_{2 \times 2} + d_x(k)\sigma_x + d_y(k)\sigma_y + d_z(k)\sigma_z, \tag{2.13}$$

where

$$\begin{cases} d_0(k) &= \frac{\epsilon_s + \epsilon_p}{2} + (-t_s + t_p)\cos(ka), \\ d_x(k) &= 0, \\ d_y(k) &= -2V_{sp}\sin(ka), \\ d_z(k) &= \frac{\epsilon_s - \epsilon_p}{2} + (-t_s - t_p)\cos(ka). \end{cases} \quad (2.14)$$

Naively, we might choose the form of eigenvector as

$$|m\rangle = \left[ \frac{2(d_y^2 + d_z^2) - 2d_z\sqrt{d_y^2 + d_z^2}}{d_y^2} \right]^{-0.5} \begin{pmatrix} i(\sqrt{dy^2+dz^2}-dz) \\ \frac{dy}{1} \end{pmatrix}; \quad (2.15)$$

however, we will encounter some divergent integrand in the later calculation of topological invariants by this eigenvector, which urges us to chose a more symmetric version of eigenvector. To figure out this eigenvector  $|m(k)\rangle$ , we unitary transform the Hamiltonian  $H$  to get  $\tilde{H}$  first. Then calculate the eigenvector  $|\widetilde{m}(k)\rangle$ . Finally we can get the  $|m(k)\rangle$  back by inverse unitary transformation.

$$\begin{aligned} H|m\rangle &= E|m\rangle, \\ HU^{-1}U|m\rangle &= EU^{-1}U|m\rangle, \\ UHU^{-1}U|m\rangle &= EU|m\rangle, \\ \tilde{H}|\widetilde{m}\rangle &= E|\widetilde{m}\rangle. \end{aligned} \quad (2.16)$$

where  $|\widetilde{m}\rangle = U|m\rangle$ ,  $|m\rangle = U^{-1}|\widetilde{m}\rangle$  and  $U = U^{-1} = \frac{1}{\sqrt{2}}((1, 1), (1, -1))$ .

For the result

$$\widetilde{H}(k) = \begin{pmatrix} d_0 & dz + id_y(k) \\ dz - id_y & d_0(k) \end{pmatrix}, \quad (2.17)$$

$$|\widetilde{m}(k)\rangle = \frac{1}{\sqrt{2}} \begin{pmatrix} \frac{-dz - id_y}{\sqrt{dy^2 + dz^2}} \\ 1 \end{pmatrix}, \quad (2.18)$$

$$|m(k)\rangle = \frac{1}{\sqrt{2}} \begin{pmatrix} \frac{-dz - id_y + \sqrt{dy^2 + dz^2}}{\sqrt{dy^2 + dz^2}} \\ \frac{-dz - id_y - \sqrt{dy^2 + dz^2}}{\sqrt{dy^2 + dz^2}} \end{pmatrix}. \quad (2.19)$$

We can check whether this is an eigenvector of the bulk hamiltonian or not by calculating  $(H - E)|m\rangle \stackrel{?}{=} 0$ . Substituting the expressions of the Hamiltonian, eigenenergies and  $|m\rangle$  into the above criteria, we can get

$$\frac{1}{2\sqrt{dy^2 + dz^2}} \begin{pmatrix} (dz + \sqrt{dy^2 + dz^2})(-dz - id_y + \sqrt{dy^2 + dz^2}) - id_y(-dz - id_y) + id_y\sqrt{dy^2 + dz^2} \\ -id_ydz - dy^2 + id_y\sqrt{dy^2 + dz^2} + dz^2 + id_ydz - (dy^2 + dz^2) - id_y\sqrt{dy^2 + dz^2} \end{pmatrix} \stackrel{M_{ma}}{=} \begin{pmatrix} 0 \\ 0 \end{pmatrix} \quad (2.20)$$

which turns out it is.

Until now, we have obtained the orbital part of the eigenstates. For the complete eigenstates, we can write it (conduction band) as

$$\begin{aligned} |k, c\rangle &= c_{c,k}^+ |vac\rangle, \\ &= m_{11}(k)c_k^+ |vac\rangle + m_{21}(k)p_k^+ |vac\rangle, \\ &= m_{11}(k)|\chi_{s,k}\rangle + m_{21}(k)|\chi_{p,k}\rangle, \end{aligned} \quad (2.21)$$

where  $|\chi_{s,k}\rangle$  is a Bloch state for the s band and  $|\chi_{p,k}\rangle$  is a Bloch state for the p band, while  $m_{11}$  and  $m_{21}$  are the elements of eigenvectors.

Since we focus on the Wannier exciton whose Bohr radius is much larger than hydrogen atom due to a large dielectric constant (mainly in 3D) and small effective masses, we can simplify the Bloch wave function  $|\chi_{s,k}\rangle$  and  $|\chi_{p,k}\rangle$  as a plane wave  $e^{ikx}$ . Therefore, we can rewrite  $|k, v\rangle$  as the orbital part tensor-multiplied by plane wave part as

$$\begin{aligned} |k, v\rangle &= |m(k)\rangle \otimes |k\rangle, \\ \langle x|k, v\rangle &= |m(k)\rangle \otimes e^{ikx}. \end{aligned} \quad (2.22)$$

### 2.3 Topological Invariant

When a system travels adiabatically, its  $n$ th eigenstate will gain a phase factor contributed from both time evolution and the variation of the instantaneous eigenstate. In the early stage of quantum mechanics, people believed that the second-part contribution could be canceled and absorbed by redefining the eigenstate. It was Berry [29] who explicitly proved that such a phase could not be canceled if the evolution of Hamiltonian is cyclic. It comes from the geometrical properties of the parameter space of the Hamiltonian and thus cannot be canceled and is invariant. This new phase (geometric phase) was first predicated in the atomic system by Aharonov and Bohm in 1959 [30]. Triggered by the integer quantum Hall effect, the idea of a geometric phase has been introduced into the solid-state system by TKNN, Niu, Zak [5] [31] [32] and others.

Since we now know the form of orbital part  $|m(k)\rangle$ , we can use the formula of the Berry phase in a solid system to calculate the winding number [28] [33], which can be expressed as a path integral in the parameter space

$$\gamma = \frac{i}{2\pi} \int_{-\pi}^{+\pi} dk \langle m(k) | \frac{\partial}{\partial k} | m(k) \rangle. \quad (2.23)$$

In order to do some concrete calculation, we have to assign the strength of the on-site terms and hopping terms. Without losing generality, for the on-site terms, we can choose  $\epsilon_s = 0$ ,  $\epsilon_p = \epsilon$  since only the relative value is important. For the hopping terms we can choose  $t_p = -4t_s = 4t$ ,  $V_{sp} = V$  since the p-p bond is stronger than s-s bond and flips the sign. Then the parameters in  $H_0$  read as

$$\begin{cases} d_0(k) &= \frac{\epsilon}{2} + 5t\cos(ka), \\ d_x(k) &= 0, \\ d_y(k) &= -2V\sin(ka), \\ d_z(k) &= -\frac{\epsilon}{2} - 3t\cos(ka). \end{cases} \quad (2.24)$$

For the dimensionless purpose, we can divide the whole Hamiltonian by  $t$  and get

$$\begin{cases} d_0(k) &= \bar{\epsilon} + 5\cos(\bar{k}), \\ d_x(k) &= 0, \\ d_y(k) &= -2\bar{V}\sin(\bar{k}), \\ d_z(k) &= -\bar{\epsilon} - 3\cos(\bar{k}). \end{cases} \quad (2.25)$$

where  $\bar{\epsilon} = \frac{\epsilon}{2t}$ ,  $\bar{V} = \frac{V}{t}$  and  $\bar{k} = ka$ .

As shown in Fig.2, we can get different winding number under different parameters where 0 represents for the trivial phase.

We can visualize whether the system has a non-trivial topological behavior by the path of vector  $d(k)$  on the dx-dy plane. If the origin point is included inside the loop of the path, the system will has non-trivial winding number as shown in Fig. 3.

## 3 Excitons with bare Coulomb interaction

This section will phenomenologically introduce the basic idea of a Wannier exciton living in the semiconductor, while the binding energy will be calculated with bare Coulomb interaction in 3D. It can be described as electron-hole pairs bounded by Coulomb attraction, which is similar to a huge hydrogen atom.

### 3.1 The physical picture

As shown in Fig.4 [20], an electron-hole pair can be created by exciting one electron from the valence band to conduction band in the semiconductor.

After the excitation in such materials creates plane wave functions for both electron and hole, the exciton formation localizes the pair by Coulomb interaction. At the first glance, this looks weird since the Coulomb interaction is repulsive between electrons, and thus, no bound state can be formed. Nevertheless, we should notice that when we



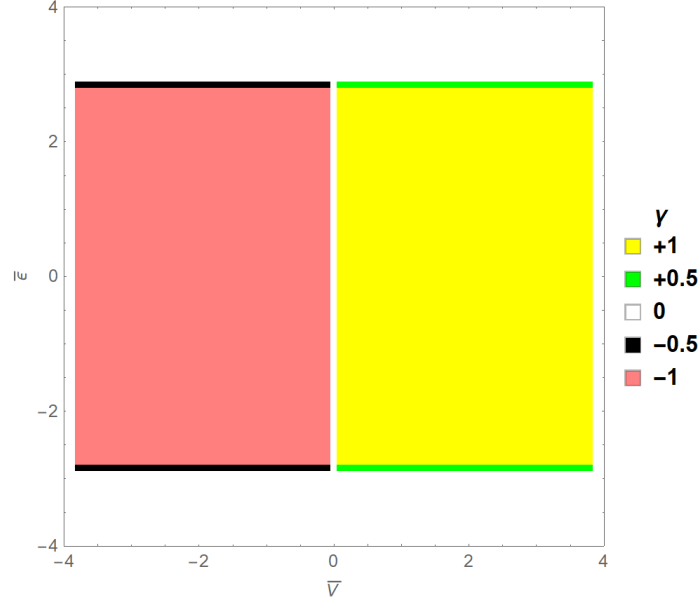


Figure 2: Phase diagram of the s-p 1D chain model. The winding number of the bulk momentum-space Hamiltonian  $H(k)$  can be +1 if  $\bar{V} > 0$  &  $-3 < \bar{\epsilon} < 3$  or -1 if  $\bar{V} < 0$  &  $-3 < \bar{\epsilon} < 3$ . If  $-3 < \bar{\epsilon}$  or  $-\bar{\epsilon} > 0$ , the winding number is 0.

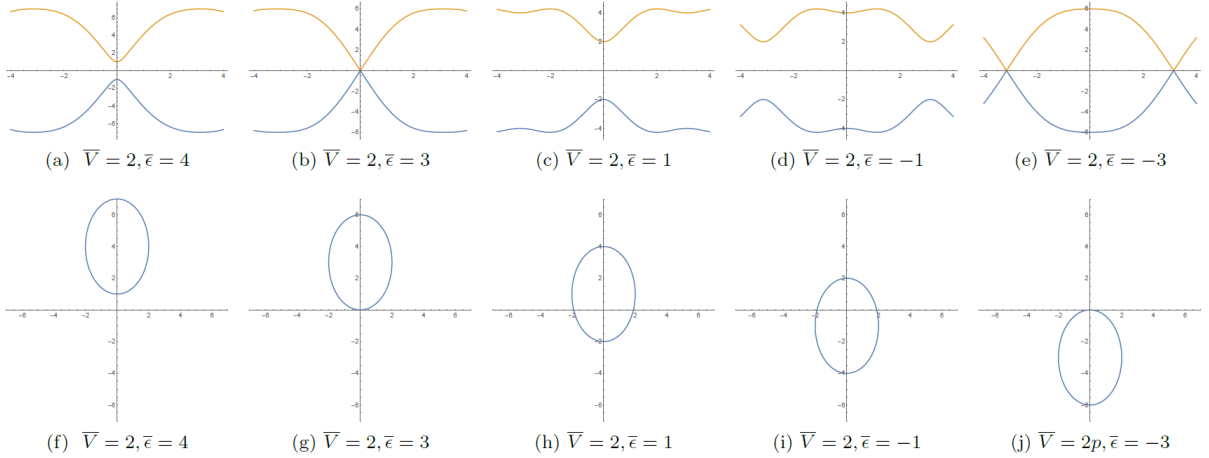


Figure 3: a to e :the dispersion relation under different parameters. f to j :the winding feature around the degenerate point under different parameters.

introduce the hole representation, we revert the charge from  $-e$  to  $+e$  and  $k_h = -k_v$ . Moreover, by requiring energy of the absence of electron in state  $k$  equals to the negative energy of of electron in state  $k$ , we can define the effective mass of hole also as positive. A good way to remember this notation is by thinking of pushing a hole away from the top of valance band is equivalent of pulling a electron back to the top [2]. As a result in Eq. 3.1, the energy of system increase when we push a hole away from the top and vice versa.

$$E_{hole} = constant + \frac{|k - k_{max}|^2}{2m_{hole}}, \quad (3.1)$$

where  $k_{max}$  the top of the valence band and  $m_{hole}$  is the mass for the hole. Since now we have both the positive charge and negative charge, the bound state can be formed by Coulomb attraction. We will calculate the energy in section 3.2.

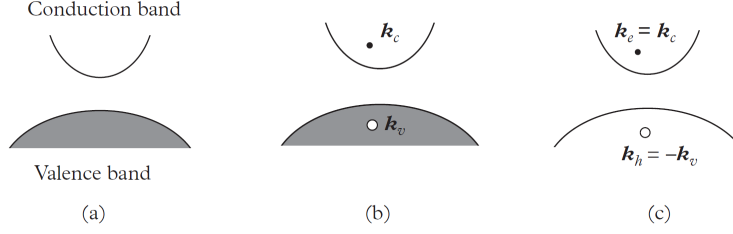


Figure 4: (a.) At  $T=0K$ , the semiconductor is a band insulator where the valance band is fully filled, and the conduction band is empty. (b.) By absorption of a photon or thermal perturbations, the electron will jump from the valance band to the conduction band and leave a 'hole' behind. (c.) We can redefine the 'hole' as a new particle and remove the Fermi sea; therefore, the model can be simplified as a two-particle problem.

### 3.2 Hydrogen-like eigenenergies

Since the attraction between an electron-hole pair forms exciton, analogically, we can apply it to the well-known two-body problem (e.g., hydrogen atom). We first treat it by first quantization, where we can write down the Schrödinger equation as

$$H = \frac{p_e^2}{2m_e} + \frac{p_h^2}{2m_h} - \frac{e^2}{4\pi\epsilon_0|r_e - r_h|}. \quad (3.2)$$

It is convenient to treat the two-body problem in the center-of-mass frame. We define the center-of-mass momentum of the pair as  $P = p_e + p_h$  and relative motion momentum as  $p = \gamma_h p_e - \gamma_e p_h$ . Then the Schrödinger equation can be written as

$$H = \frac{P^2}{2M} + \frac{p^2}{2\mu} - \frac{e^2}{4\pi\epsilon_0|r|}, \quad (3.3)$$

where  $M$  is the total mass and  $\mu$  is the reduced mass, is the relative constant of the semiconductor. Now we can split the wavefunction into a center-of-mass part which is a plane wave and a relative part which is the solution of a central potential problem as

$$\psi(r_e, r_h) = \frac{e^{iQ_i R}}{V^{\frac{1}{2}}} \phi_{\nu_i}(r), \quad (3.4)$$

where the volume is  $V$ ;  $\phi_{\nu_i}(r)$  is a solution of the *Schrödinger* equation for the relative part. In real space, it can be written as

$$\left( \frac{\hat{p}^2}{2\mu} - \frac{e^2}{4\pi\epsilon_0|r|} \right) \phi_{\nu_i}(r) = E_{\nu_i} \phi_{\nu_i}(r). \quad (3.5)$$

The energy of such an equation is well-known as [18]

$$E_{\nu_i}(n) = -\frac{\frac{\mu}{m^2} Ry}{n^2}, \quad (3.6)$$

where  $Ry$  is the Rydberg unit of energy. Typically, the exciton energy is 10 times smaller than hydrogen atom since  $\mu$  is around 10 times smaller than a free electron mass in 1D [20].

We can also write Eq. 3.5 in momentum space. We do this because it is more convenient to calculate the energy numerically in momentum space since the Coulomb interaction is not bare in the real system. As we will show, such a momentum form can be derived from a microscopic picture.

$$\frac{p^2}{2\mu} \phi_{\nu_i,p} - \frac{1}{V} \sum_q V_q \phi_{\nu_i,p+q} = E_{\nu_i} \phi_{\nu_i,p} \quad (3.7)$$

where the  $V_q$  is the Fourier transformation of  $\frac{e^2}{4\pi\epsilon_0|r|}$ .

## 4 Coulomb matrix elements in 1D chain

### 4.1 Hamiltonian

Unlike the bare Coulomb interaction from last section, we come back to our 1D chain model again and wish to figure out the exact Coulomb interaction matrix. To achieve this goal, we introduce particle-particle interaction into our model by adding a term as

$$H_{int} = H_{coulomb} = \frac{1}{2} \int dx \int dx' \Psi^\dagger(x) \Psi^\dagger(x') V(x-x') \Psi(x') \Psi(x). \quad (4.1)$$

Using the Wannier functions, we can expand the field operator as

$$\begin{aligned} \Psi(x) &= \sum_{n,i} a_{n,i} w_n(x-x_i), \\ \Psi(x') &= \sum_{n',i'} a_{n',i'} w_{n'}(x'-x_{i'}), \\ \Psi^\dagger(x) &= \sum_{m,j} a_{m,j}^+ w_m^*(x-x_j), \\ \Psi^\dagger(x') &= \sum_{m',j'} a_{m',j'}^+ w_{m'}^*(x'-x_{j'}). \end{aligned} \quad (4.2)$$

By plugging the relation above into the  $H_{int}$ , we can rewrite it as

$$H_{int} = \frac{1}{2} \sum_{\substack{j,j';i',i \\ m,m';n',n}} a_{j,m}^+ a_{j',m'}^+ a_{i',n'} a_{i,n} U_{j,j';i',i; m,m';n',n}, \quad (4.3)$$

where

$$U_{j,j';i',i; m,m';n',n} = \int dx \int dx' w_m^*(x-x_j) w_{m'}^*(x'-x_{j'}) V(x-x') w_n(x-x_i) w_{n'}(x'-x_{i'}). \quad (4.4)$$

As an example, we write out the s-s term explicitly

$$\begin{aligned} H_{int} &= \frac{1}{2} \sum_{\substack{j,j';i',i \\ m,m';n',n}} U_{j,j';i',i; m,m';n',n} a_{j,m}^+ a_{j',m'}^+ a_{i',n'} a_{i,n}, \\ &= \frac{1}{2} \sum_{j,j'} U_{j,j';j',j} a_{j,s}^+ a_{j',s}^+ a_{j',s} a_{j,s}, \\ &= \frac{1}{2} \sum_{j,j'} U_{j,j';j',j} c_j^+ c_{j'}^+ c_{j'} c_j. \end{aligned} \quad (4.5)$$

After the Fourier transformation

$$\begin{aligned}
H_{int} &= \frac{1}{2} \sum_{j,j'} U_{j,j';j',j} \frac{1}{N^2} \sum_{k_1,k_2,k_3,k_4} e^{-ik_1x_j} e^{-iL_2x_{j'}} e^{+ik_3x_{j'}} e^{+ik_4x_j} c_{k_1}^+ c_{k_2}^+ c_{k_3} c_{k_4}, \\
&= \frac{1}{2} \sum_{j,j'} U_{j,j';j',j} \frac{1}{N^2} \sum_{k_1,k_2,k_3,k_4} e^{-ix_j(k_1-k_4+k_2-k_3)} \cdot e^{-ix_{j'}(k_2-k_3)} \cdot e^{ix_j(k_2-k_3)} c_{k_1}^+ c_{k_2}^+ c_{k_3} c_{k_4}, \\
&= \frac{1}{2} \frac{1}{N} \sum_{j'} U_{j,j';j',j} \sum_{k_1,k_2,k_3,k_4} e^{i(x_j-x_{j'})(k_2-k_3)} \cdot \delta_{k_1-k_4+k_2-k_3=0} \cdot c_{k_1}^+ c_{k_2}^+ c_{k_3} c_{k_4}, \\
&= \frac{1}{2} \frac{1}{N} \sum_{j'} U((j-j')R_0) \sum_{k_1,k_2,k_3,k_4} e^{i(x_j-x_{j'})(k_2-k_3)} \cdot \delta_{k_1-k_4+k_2-k_3=0} \cdot c_{k_1}^+ c_{k_2}^+ c_{k_3} c_{k_4}, \\
&= \frac{1}{2} \frac{1}{N} \sum_{\tilde{j}=-\frac{N}{2}}^{\tilde{j}=\frac{L}{2}} U(\tilde{j}R_0) \sum_{k_1,k_2,k_3,k_4} e^{i(\tilde{j}R_0)(k_2-k_3)} \cdot \delta_{k_1-k_4+k_2-k_3=0} \cdot c_{k_1}^+ c_{k_2}^+ c_{k_3} c_{k_4}, \\
&= \frac{1}{2} \frac{1}{N} \sum_{k_1,k_2} \sum_q U(q) \cdot c_{k_1+q}^+ c_{k_2-q}^+ c_{k_2} c_{k_1},
\end{aligned} \tag{4.6}$$

where

$$\begin{aligned}
U(q) &= \sum_{\tilde{j}=-\frac{N}{2}}^{\tilde{j}=\frac{N}{2}} U(\tilde{j}R_0) e^{i(k_2-k_3)(\tilde{j}R_0)}, \\
&= \sum_{\tilde{j}=-\frac{N}{2}}^{\tilde{j}=\frac{N}{2}} U(\tilde{j}R_0) e^{i(q)(\tilde{j}R_0)}, \\
&= \sum_{\tilde{j}=-\frac{N}{2}}^{\tilde{j}=\frac{N}{2}} U(x_{\tilde{j}}) e^{i(q)(x_{\tilde{j}})}, \\
&= \frac{1}{R_0} \int_{x_{\tilde{j}}=-\infty}^{x_{\tilde{j}}=+\infty} U(x_{\tilde{j}}) e^{i(q)(x_{\tilde{j}})} dx_{\tilde{j}}.
\end{aligned} \tag{4.7}$$

## 4.2 Matrix elements in real space

We ignore the prefactor  $\frac{e^2}{4\pi\epsilon_0}$  before Coulomb interaction for a while. In order to get the matrix element of Coulomb interaction, we need to integrate the term

$$U_{j,j';i',i} = \int dx \int dx' w_m^*(x-x_j) w_m^*(x'-x_{j'}) V(x-x') w_n'(x'-x_{i'}) w_n(x-x_i). \tag{4.8}$$

Because the direct terms within two atoms dominate the Coulomb interaction, we ignore the exchange terms and focus on direct terms  $U_{j,j';j',j}$  s. We introduce a new notation to emphasize the density of wavefunctions of electron 1 and electron 2 as

$$\langle a^2 | \frac{1}{r_{12}} | b^2 \rangle = - \int dx \int dx' |w_m(x-x_j)|^2 V(x-x') |w_n(x-x_j)|^2, \tag{4.9}$$

where "a" represents the wavefunction for atom "a" and "b" represents the wavefunction for atom "b".

As shown in Fig. 5, this integrand can be viewed as two parts. The first part is the Coulomb potential induced by the charge distribution of electron 2, namely the result of all elementary electrostatic potential contributions at  $r_1$  due to the continuously varying charge distribution of electron 2. The second part represents the process of how electron 1 feels the cloud of electron 2. Hence

$$\begin{aligned}
&\langle a^2 | \frac{1}{r_{12}} | b^2 \rangle \\
&= \int dr_1 J_B(r_{1B}) a^2(r_{1A}),
\end{aligned} \tag{4.10}$$

where

$$J_B(r_{1B}) = \int dr_{2B} \frac{b^2(r_{2B})}{r_{12}}. \quad (4.11)$$

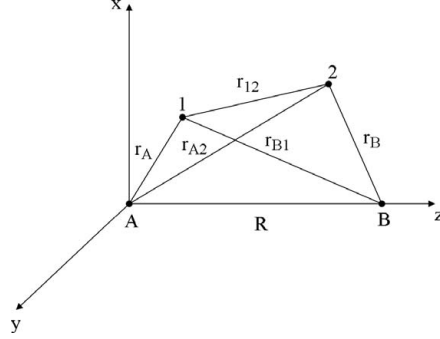


Figure 5: The number 1 and 2 represent the position of electron 1 and electron 2. Letter A and B mean the positions of two atomic nuclei.

As the simplest example, we consider the s-wave case.

$$J_{1s} = \int dr_2 \frac{[1s(r_2)]^2}{r_{12}}. \quad (4.12)$$

In order to solve such an integral, we need to express the  $\frac{1}{r_{12}}$  as

$$\frac{1}{r_{12}} = \sum_{l=0}^{\infty} \frac{4\pi}{2l+1} \frac{r_{<}^l}{r_{>}^{l+1}} \sum_{m=-l}^{+l} Y_{lm}(\Omega_1) Y_{lm}(\Omega_2), \quad (4.13)$$

where

$$\begin{aligned} r_{<} &= \min(r_1, r_2), \\ r_{>} &= \max(r_1, r_2), \\ 1s(r) &= R_{10} Y_{00}, \\ 1s(r) &= (4c^3)^{\frac{1}{2}} e^{-cr} \sqrt{\frac{1}{4\pi}}. \end{aligned} \quad (4.14)$$

Inserting Eq. 4.14 into  $J_{1s}$ , we can get

$$\begin{aligned} J_{1s}(r_1) &= \int dr_2 r_2^2 d\Omega_2 4c^3 e^{-2cr_2} Y_{00}^2(\Omega_2) \cdot \sum_l \sum_m \frac{4\pi}{2l+1} Y_{lm}(\Omega_1) Y_{lm}(\Omega_2) \frac{r_{<}^l}{r_{>}^{l+1}}, \\ &= \sum_l \sum_m 4c^3 \frac{4\pi}{2l+1} Y_{lm}(\Omega_1) Y_{00}(\Omega_1) \int d\Omega_2 Y_{lm}(\Omega_2) Y_{00}(\Omega_2) \\ &\quad \left\{ \frac{1}{r_1^{l+1}} \int_0^{r_1} dr_2 r_2^2 e^{-2cr_2} r_2^l + r_1^l \int_{r_1}^{\infty} dr_2 r_2^2 e^{-2cr_2} \frac{1}{r_2^{l+1}} \right\}, \\ &\stackrel{l=m=0}{=} 4c^3 \cdot 4\pi \cdot \left( \frac{1}{\sqrt{4\pi}} \right)^2 \cdot 1 \cdot \left\{ \frac{1}{r_1} \int_0^{r_1} dr_2 r_2^2 e^{-2cr_2} + \int_{r_1}^{\infty} dr_2 r_2 e^{-2cr_2} \right\}, \\ &\stackrel{Mma}{=} \frac{1}{r_1} - \frac{1}{r_1} e^{-2cr_1} (1 + cr_1). \end{aligned} \quad (4.15)$$

After we get the expression of  $J_{1s}$ , we need to calculate  $\int dr_1 J_B(r_{1B}) a^2(r_{1A})$  with the help of the spheroidal coordinates [34]

$$r_{1A} \rightarrow \frac{R}{2}(\mu + \nu), \quad (4.16)$$

$$r_{1B} \rightarrow \frac{R}{2}(\mu - \nu), \quad (4.17)$$

$$\cos(\theta_A) \rightarrow \frac{1 + \mu\nu}{\mu + \nu}, \quad (4.18)$$

$$dr \rightarrow \left(\frac{R}{2}\right)^3 (\mu^2 - \nu^2) d\mu d\nu d\phi. \quad (4.19)$$

After a coordinate transformation

$$\int dr_1 J_{1B}(r_1) a^2(r_1) \quad (4.20)$$

$$= dr_1 \cdot \left\{ \frac{1}{r_{1B}} - \frac{1}{r_{1B}} e^{-2cr_{1B}} (1 + cr_{1B}) \right\} \cdot \left\{ (4c^3)^{\frac{1}{2}} \cdot c^3 \cdot \sqrt{\frac{1}{4\pi}} e^{cr_{1A}} \right\}^2. \quad (4.21)$$

We will write the expression for  $U_{s,s;s,s}(\rho)$  later. For  $p_\sigma - p_\sigma$  interaction, we have

$$2p_\sigma = R_{21} Y_{10} = \frac{2\sqrt{3}}{3} c^{\frac{5}{2}} \cdot r \cdot e^{-cr} \cdot \sqrt{\frac{3}{4\pi}} \cos(\theta), \quad (4.22)$$

$$J_{p_\sigma - p_\sigma} = \int dr_2 \frac{[2p_\sigma(r_2)]^2}{r_{12}}, \quad (4.23)$$

$$= \int dr_2 r_2^2 d\Omega_2 \frac{4}{3} c^5 \cdot r_2^2 \cdot e^{-2cr_2} [Y_{10}(\Omega_2)]^2 \cdot \sum_l \sum_m \frac{4\pi}{2l+1} Y_{lm}(\Omega_1) Y_{lm}(\Omega_2) \frac{r_{<}^l}{r_{>}^{l+1}}. \quad (4.24)$$

Unlike the s-wave situation, we need a step to rewrite  $[Y_{lm}(\Omega_2)]^2$  as first order of spherical harmonics

$$[Y_{lm}(\Omega_2)]^2 = \frac{3}{4\pi} \cos^2(\theta_2) = c_{0,0} Y_{00}(\theta_2, \phi_2) + c_{2,0} Y_{20}(\theta_2, \phi_2), \quad (4.25)$$

$$= c_{0,0} \cdot \sqrt{\frac{1}{4\pi}} + c_{2,0} \cdot \frac{1}{4} \sqrt{\frac{5}{\pi}} \cdot (3\cos^2(\theta_2) - 1), \quad (4.26)$$

$$= \sqrt{\frac{1}{4\pi}} \cdot \sqrt{\frac{1}{4\pi}} + \sqrt{\frac{1}{5\pi}} \cdot \frac{1}{4} \sqrt{\frac{5}{\pi}} \cdot (3\cos^2(\theta_2) - 1), \quad (4.27)$$

$$= \sqrt{\frac{1}{4\pi}} \cdot Y_{00}(\Omega_2) + \sqrt{\frac{1}{5\pi}} Y_{20}(\Omega_2). \quad (4.28)$$

$$(4.29)$$

Now

$$J_{p_\sigma - p_\sigma} = \int dr_2 r_2^2 d\Omega_2 \frac{4}{3} c^5 \cdot r_2^2 \cdot e^{-2cr_2} \left[ \sqrt{\frac{1}{4\pi}} \cdot Y_{00}(\Omega_2) + \sqrt{\frac{1}{5\pi}} Y_{20}(\Omega_2) \right] \cdot \sum_l \sum_m \frac{4\pi}{2l+1} Y_{lm}(\Omega_1) Y_{lm}(\Omega_2) \frac{r_{<}^l}{r_{>}^{l+1}}, \quad (4.30)$$

$$= \frac{4c^5}{3} \left[ \int_0^{r_1} \frac{1}{r_1} e^{-2cr_2} \cdot r_2^4 dr_2 + \int_{r_1}^\infty e^{-2cr_2} \cdot r_2^3 dr_2 \right] + \frac{4c^5}{3} \cdot \frac{1}{5} \cdot (3\cos^2(\theta_1) - 1) \left[ \int_0^{r_1} \frac{1}{r_1^3} e^{-2cr_2} r_2^6 dr_2 + \int_{r_1}^\infty r_1^2 \cdot e^{-2cr_2} r_2 dr_2 \right]. \quad (4.31)$$

Using Mathematica, we get the expression of  $U(\rho)$  as

$$U_{classical} = -\frac{1}{\rho}, \quad (4.32)$$

$$U_{ss-ss}(\rho) = -\frac{1 - e^{-2\rho} \left( \frac{\rho^3}{6} + \frac{3\rho^2}{4} + \frac{11\rho}{8} + 1 \right)}{\rho}, \quad (4.33)$$

$$U_{sp-ps}(\rho) = \frac{1}{20}e^{-2\rho}\rho^4 + \frac{41}{120}e^{-2\rho}\rho^3 + \frac{3e^{-2\rho}}{\rho^3} - \frac{3}{\rho^3} + \frac{301}{240}e^{-2\rho}\rho^2 + \frac{6e^{-2\rho}}{\rho^2} + \frac{25}{8}e^{-2\rho}\rho + \frac{89e^{-2\rho}}{16} + \frac{7e^{-2\rho}}{\rho} - \frac{1}{\rho}, \quad (4.34)$$

$$U_{pp-pp}(\rho) = -\frac{\frac{54}{\rho^4} + \frac{6}{\rho^2}}{\rho} + \frac{e^{-2\rho} \left( -\frac{\rho^7}{140} - \frac{47\rho^6}{840} - \frac{19\rho^5}{70} - \frac{893\rho^4}{840} - \frac{54}{\rho^4} - \frac{24209\rho^3}{6720} - \frac{108}{\rho^3} - \frac{6411\rho^2}{640} - \frac{114}{\rho^2} - \frac{30731\rho}{1280} - \frac{84}{\rho} - 49 \right) + 1}{\rho}. \quad (4.35)$$

According to Fig. 6, we get a finite value when  $\rho$  is 0 compared with the divergent behavior of bare Coulomb behavior. Meanwhile, all of the functions  $U$  approach to  $-\frac{1}{\rho}$  when  $\rho$  goes to  $\infty$  just like bare Coulomb behavior.

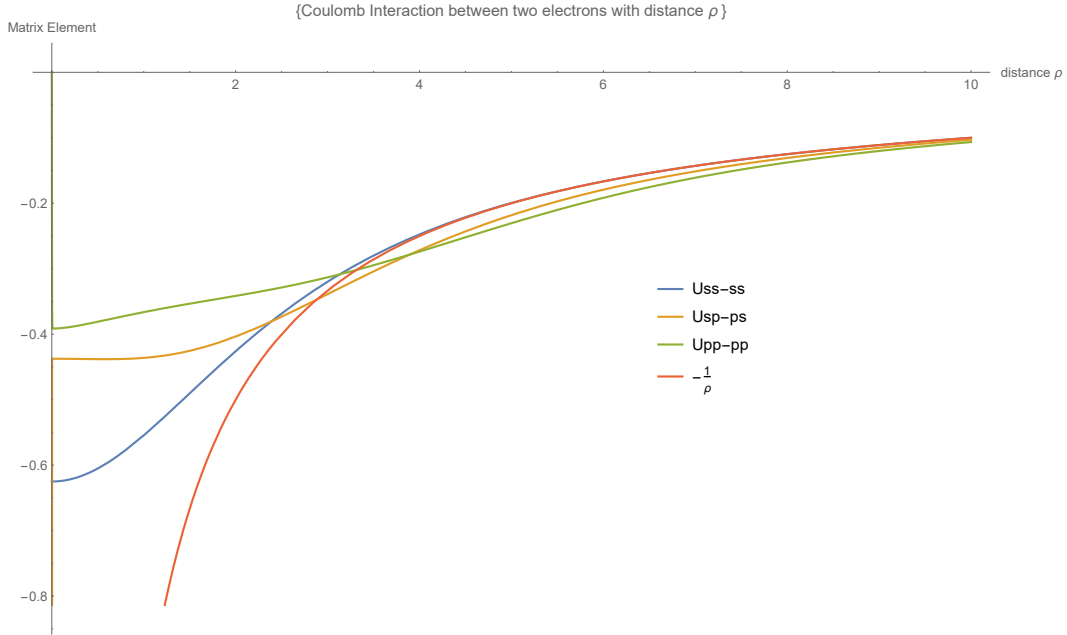


Figure 6: Matrix elements  $U$  vs. distance of atomic nuclei. Here the length scale is set as Bohr radius of Hydrogen atom  $a_0$  while the energy scale is set as Rydberg unit of energy. Therefore  $\frac{a}{0}$  represents the nearest neighbor. While there is some instability when drawing such a function in Mathematica, all the four matrix elements are actually finite at  $\rho=0$ .

The results coincide with precious work by K Ruedenberg [35]. We can check the asymptotic behavior towards zero by Taylor expansion as

$$U_{ss-ss}(\rho) = -\frac{5}{8} + \frac{\rho^2}{12} - \frac{\rho^4}{60} + O(\rho^6), \quad (4.36)$$

$$U_{sp-ps}(\rho) = -\frac{7}{16} - \frac{\rho^2}{240} + \frac{\rho^4}{140} + O(\rho^6), \quad (4.37)$$

$$U_{pp-pp}(\rho) = -\frac{501}{1280} + \frac{361\rho^2}{4480} - \frac{5\rho^3}{42} + \frac{73\rho^4}{640} - \frac{5\rho^5}{63} + O(\rho^6). \quad (4.38)$$

$$(4.39)$$

We can also check the asymptotic behavior towards infinity by Taylor expansion as

$$U_{ss-ss}(\rho) = e^{-2\rho+O\left(\left(\frac{1}{\rho}\right)^7\right)} \left( \frac{\rho^2}{6} + \frac{3\rho}{4} + \frac{11}{8} + \frac{1}{\rho} + O\left(\left(\frac{1}{\rho}\right)^3\right) \right) + \left( -\frac{1}{\rho} + O\left(\left(\frac{1}{\rho}\right)^3\right) \right), \quad (4.40)$$

$$U_{sp-ps}(\rho) = e^{-2\rho+O\left(\left(\frac{1}{\rho}\right)^{11}\right)} \left( \frac{\rho^4}{20} + \frac{41\rho^3}{120} + \frac{301\rho^2}{240} + \frac{25\rho}{8} + \frac{89}{16} + \frac{7}{\rho} + \frac{6}{\rho^2} + O\left(\left(\frac{1}{\rho}\right)^3\right) \right) + \left( -\frac{1}{\rho} + O\left(\left(\frac{1}{\rho}\right)^3\right) \right), \quad (4.41)$$

$$U_{pp-pp}(\rho) = e^{-2\rho+O\left(\left(\frac{1}{\rho}\right)^{11}\right)} \left( \frac{\rho^6}{140} + \frac{47\rho^5}{840} + \frac{19\rho^4}{70} + \frac{893\rho^3}{840} + \frac{24209\rho^2}{6720} + \frac{6411\rho}{640} + \frac{30731}{1280} + \frac{49}{\rho} + \frac{84}{\rho^2} + O\left(\left(\frac{1}{\rho}\right)^3\right) \right) + \left( -\frac{1}{\rho} + O\left(\left(\frac{1}{\rho}\right)^3\right) \right). \quad (4.42)$$

### 4.3 Matrix elements in momentum space

By Fourier transformation, we can get the Matrix element in momentum space as

$$U_{classical} = \frac{\log(|q|) + \gamma}{\pi}, \quad (4.43)$$

$$U_{ss-ss}(q) = \frac{-3 \log(q^2 + 4) + \frac{4(3q^4 + 30q^2 + 88)}{(q^2 + 4)^3} + 6 \log(q)}{6\pi}, \quad (4.44)$$

$$U_{sp-ps}(q) = \frac{(60 - 90q^2) \log(q) + 15(3q^2 - 2) \log(q^2 + 4) - \frac{4(45q^{10} + 780q^8 + 5100q^6 + 14720q^4 + 13984q^2 - 16000)}{(q^2 + 4)^5}}{60\pi}, \quad (4.45)$$

$$U_{pp-pp}(q) = \frac{210(2 - 3q^2)^2 \log(q) - 105(2 - 3q^2)^2 \log(q^2 + 4)}{840\pi} + \frac{(3526024q^6 + 4090240q^4 - 1901568q^2 + 15(7(9q^4 + 222q^2 + 2260)q^2 + 83934)q^8 - 7907840)q^2 + 3979264}{210\pi(q^2 + 4)^7}. \quad (4.46)$$

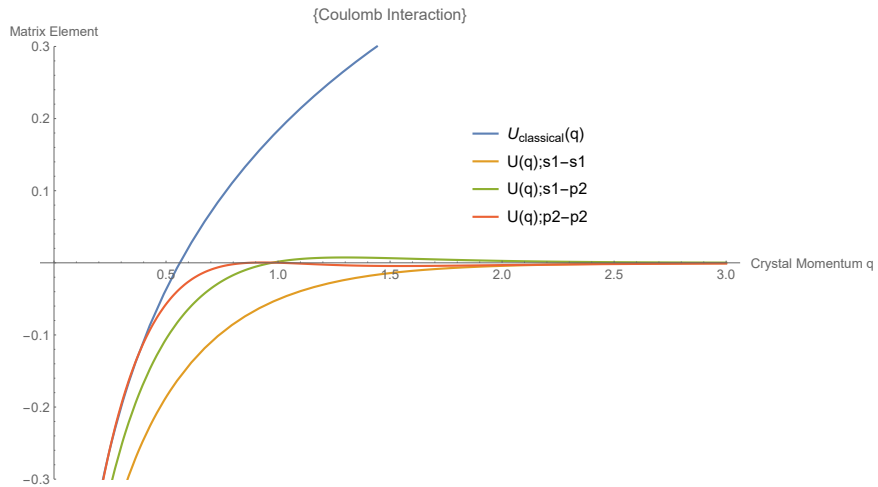


Figure 7: Coulomb matrix element in momentum space vs. crystal momentum  $q$ . Here the momentum scale is set as inverse of the Bohr radius as  $\frac{1}{a_0}$  while the energy scale is set as the Rydberg unit of energy.



We can check the asymptotic behavior in the low-momentum limits by Taylor expansion as

$$U_{classical}(q) = \frac{\log(|q|) + \gamma}{\pi}, \quad (4.47)$$

$$U_{ss-ss}(q) = \frac{12 \log(q) + 11 - 12 \log(2)}{12\pi} - \frac{q^2}{2\pi} + O(q^4), \quad (4.48)$$

$$U_{sp-ps}(q) = \frac{24 \log(q) + 25 - 24 \log(2)}{24\pi} + \frac{q^2(-120 \log(q) - 187 + 120 \log(2))}{80\pi} + O(q^4), \quad (4.49)$$

$$U_{pp-pp}(q) = \frac{1680 \log(q) + 1943 - 1680 \log(2)}{1680\pi} + \frac{q^2(-3360 \log(q) - 4981 + 3360 \log(2))}{1120\pi} + O(q^4). \quad (4.50)$$

## 5 Microscopic derivation of excitons

### 5.1 Electron-hole basis

Dropping the full valence and conduction bands description can bring benefits to us since only a few "holes" will be left in our model. This can be achieved by electron and hole operators as

$$a_{ck}^+ = a_k^+, \quad (5.1)$$

$$a_{vk}^+ = b_{-k}^+. \quad (5.2)$$

$$(5.3)$$

### 5.2 Non-interacting part

Starting with the one-body Hamiltonian, we can convert it into an electron-hole basis as

$$H_0 = \sum_k \{ \epsilon_{ck} a_{ck}^+ a_{ck} + \epsilon_{vk} a_{vk}^+ a_{vk} \}, \quad (5.4)$$

$$= \sum_k \{ \epsilon_{ck} a_{ck}^+ a_{ck} + \epsilon_{vk} (1 - a_{vk} a_{vk}^+) \}, \quad (5.5)$$

$$= \sum_k \{ \epsilon_c a_k^+ a_k + \epsilon_{vk} + (-\epsilon_{vk}) b_k^+ b_k \}. \quad (5.6)$$

$$(5.7)$$

where we can use the effective mass approximation to represent the energy of a conduction band electron near the minimum as  $\epsilon_{ck} \simeq \epsilon_{c0} + \frac{k^2}{2m_e}$  with  $m_e > 0$ , while  $-\epsilon_{vk} \simeq -\epsilon_{v0} + \frac{k^2}{2m_h}$  with  $m_h > 0$ .

### 5.3 Interacting part

The same transformation is also applied for the Coulomb part

$$U_{cv} = 2 \cdot \frac{1}{2} \frac{1}{L} \sum_q U_q \sum_{k_1 k_2} a_{ck_1+q}^+ a_{vk_2-q}^+ a_{vk_2} a_{ck_1}, \quad (5.8)$$

$$= -\frac{1}{L} \sum_q U_q \sum_{k_1 k_2} a_{ck_1+q}^+ a_{vk_2} a_{vk_2-q}^+ a_{ck_1}, \quad (5.9)$$

$$= -\frac{1}{L} \sum_q U_q \sum_{k_1 k_2} a_{k_1+q}^+ b_{-k_2}^+ b_{-k_2+q} a_{k_1}, \quad (5.10)$$

$$\stackrel{k'_2 = -k_2+q}{=} -\frac{1}{L} \sum_q U_q \sum_{k_1 k'_2} a_{k_1+q}^+ b_{k'_2-q}^+ b_{k'_2} a_{k_1}, \quad (5.11)$$

$$\stackrel{k_2 = k'_2}{=} -\frac{1}{L} \sum_q U_q \sum_{k_1 k_2} a_{k_1+q}^+ b_{k_2-q}^+ b_{k_2} a_{k_1}, \quad (5.12)$$

$$(5.13)$$

where the prefactor  $\frac{1}{2}$  has been canceled because of the repeated summation with the choice  $n=c, m=v$  and  $n=v, m=c$ .

## 5.4 Eigenstates

It is natural to ask what is the expression of eigenstates of such a Hamiltonian:

$$H = H_e + H_h + U_{eh}, \quad (5.14)$$

where

$$H_e = \sum_k \epsilon_k^{(e)} a_k^+ a_k, \quad (5.15)$$

$$H_h = \sum_k \epsilon_k^{(h)} b_k^+ b_k, \quad (5.16)$$

$$U_{eh} = U_{cv} = -\frac{1}{L} \sum_q U_q \sum_{k_1 k_2} a_{ck_1+q}^+ b_{k_2-q}^+ b_{k_2} a_{ck_1}. \quad (5.17)$$

$$(5.18)$$

We first show that a free electron-hole pair  $|k_e k_h\rangle$  is the eigenstate of the non-interacting part of the full Hamiltonian by

$$(H_e + H_h) |k_e k_h\rangle = (\epsilon_k^{(e)} + \epsilon_k^{(h)}) |k_e k_h\rangle. \quad (5.19)$$

Now, we try to solve the full Hamiltonian under the existence of Coulomb interaction. We first write down the *Schrödinger* equation as

$$(H_e + H_h + U_{eh}) |i\rangle = E_i |i\rangle, \quad (5.20)$$

where  $|i\rangle$  is the eigensate of the full Hamiltonian. In order solve this equation, we can expand  $|i\rangle$  by inserting the projection operator of free electron-hole pair  $|k_e k_h\rangle$  as

$$|i\rangle = \sum_{k_e k_h} |k_e k_h\rangle \langle k_h k_e | i \rangle. \quad (5.21)$$

Then we can rewrite the  $|i\rangle$  with the operator language as

$$|i\rangle = \sum_{k_e k_h} a_{k_e}^+ b_{k_h}^+ |vac\rangle \langle k_h k_e | i \rangle, \quad (5.22)$$

$$= \sum_{k_e k_h} a_{k_e}^+ b_{k_h}^+ \langle k_h k_e | i \rangle |vac\rangle. \quad (5.23)$$

From Eq. (5.23), we can define the creation operator of the Wannier exciton as

$$B_i^+ = \sum_{k_e k_h} a_{k_e}^+ b_{k_h}^+ \langle k_h k_e | i \rangle. \quad (5.24)$$

Further, we would like to transform the operator  $B_i^+$  into the center-of-mass basis. To achieve that, we write the original momentum into center-of-mass part and relative motion part as

$$\langle k_h k_e | i \rangle = \langle P | Q_i \rangle \langle p | \nu_i \rangle = \langle k_e + k_h | Q_i \rangle \langle p | \nu_i \rangle = \delta_{k_e+k_h, Q_i} \langle \gamma_h k_e - \gamma_e k_h | \nu_i \rangle, \quad (5.25)$$

where  $(P, p)$  are center-of-mass and relative motion momenta of a free electron-hole pair, while  $(Q_i, \nu_i)$  are center-of-mass and relative motion momenta of an exciton. With Eq. (5.25), we can rewrite the creation operator of an exciton in state  $|i\rangle$  as

$$B_i^+ = B_{Q_i, \nu_i}^+ = \sum_p a_{p+\frac{1}{2}Q_i}^+ b_{-p+\frac{1}{2}Q_i}^+ \langle p | \nu_i \rangle, \quad (5.26)$$

$$= \sum_p f_p^{(\nu_i)} a_{p+\frac{1}{2}Q_i}^+ b_{-p+\frac{1}{2}Q_i}^+. \quad (5.27)$$

$$(5.28)$$

We can do the same thing to turn Eq. (5.20) from  $(k_e, k_h)$  basis to  $(Q_i, \nu_i)$  basis as

$$(H_e + H_h + U_{eh}) |i\rangle = \sum_{k_e k_h} (\epsilon_{k_e}^{(e)} + \epsilon_{k_h}^{(h)}) |k_e k_h\rangle \langle k_h k_e | i \rangle - \frac{1}{L} \sum_q \sum_{k_e k_h} U_q |k_e + q, k_h - q\rangle \langle k_h k_e | i \rangle, \quad (5.29)$$

$$\begin{aligned} (H_e + H_h + U_{eh}) B_{Q_i, \nu_i}^+ |vac\rangle &= \sum_p (\epsilon_{p+\frac{1}{2}Q_i}^{(e)} + \epsilon_{-p+\frac{1}{2}Q_i}^{(h)}) f_p^{(\nu_i)} a_{p+\frac{1}{2}Q_i}^+ b_{-p+\frac{1}{2}Q_i}^+ |vac\rangle \\ &\quad - \frac{1}{L} \sum_q U_q \sum_p f_p^{(\nu_i)} a_{p+q+\frac{1}{2}Q_i}^+ b_{-p-q+\frac{1}{2}Q_i}^+ |vac\rangle. \end{aligned} \quad (5.30)$$

By rewriting  $p$  into  $p-q$ , we can collect the terms in Eq. (5.30)

$$HB_{Q_i, \nu_i}^+ |vac\rangle = \sum_p \left\{ (\epsilon_{p+\frac{1}{2}Q_i}^{(e)} + \epsilon_{-p+\frac{1}{2}Q_i}^{(h)}) f_p^{(\nu_i)} - \frac{1}{L} \sum_q U_q f_{p-q}^{(\nu_i)} \right\} a_{p+\frac{1}{2}Q_i}^+ b_{-p+\frac{1}{2}Q_i}^+ |vac\rangle. \quad (5.31)$$

The above equation shows that  $B_{Q_i}^+ |vac\rangle$  is the eigenstate of the Hamiltonian, provided that the prefactor  $f$  satisfies the *Schrödinger* equation

$$(\epsilon_{p+\frac{1}{2}Q_i}^{(e)} + \epsilon_{-p+\frac{1}{2}Q_i}^{(h)}) f_p^{(\nu_i)} - \frac{1}{L} \sum_q U_q f_{p-q}^{(\nu_i)} = E_i f_p^{(\nu_i)}. \quad (5.32)$$

## 6 Eigenenergies and dispersion relation

In the section, we need to solve the Schrödinger equation to get the eigenenergies. Unlike the bare Coulomb interaction, we cannot find a way to solve the Schrödinger equation analytically with 1D effective Coulomb potential. Therefore we need to introduce a numerical method to solve it.

### 6.1 Numerical method to solve the Schrödinger equation

The key idea behind the numerical method is to discretize the Schrödinger equation into a matrix form in momentum space. After that, we can find the eigenenergies and eigenstates by the standard numerical procedure.

The Schrödinger equation reads as

$$\left[ -\frac{1}{2m} \frac{d^2}{dx^2} + V(x) \right] \psi(x) = E \psi(x). \quad (6.1)$$

By Fourier transformation

$$\psi(x) = \frac{1}{\sqrt{2\pi}} \int_{-\infty}^{+\infty} \phi(k') e^{ik'x} dk'. \quad (6.2)$$

We can rewrite the Eq. (6.2) in momentum space as

$$\frac{k^2}{2m}\phi(k) + \frac{1}{2\pi} \int_{-\infty}^{+\infty} V_{kk'}\phi(k')dk' = E\phi(k), \quad (6.3)$$

where

$$V_{kk'} = \int_{-\infty}^{+\infty} V(x)e^{-i(k-k')x}dx. \quad (6.4)$$

To convert Eq. 6.4 into a form which is suitable for a numerical calculation, we need to discretize the Hamiltonian into

$$\sum_n [u_n^2 \delta_{mn} + V_{mn}]\phi(u_n) = \sum_n H_{mn}(u_n) = E\phi(u_m), \quad (6.5)$$

where  $u_n = n \cdot \Delta k$ .

## 6.2 Numerical solution of the exciton eigenenergies in effective mass approximation

By the numerical method introduced by the section 6.1, we can solve the Eq. (6.13) for the exciton numerically. For simplicity, we can choose  $U_q = U_{ss-ss}(q)$  since  $U_{ss-ss}(q)$ ,  $U_{sp-ps}(q)$  and  $U_{pp-pp}(q)$  share the same asymptotic behavior at  $q=0$  which characterizes the long-wave behavior of the system.

We first use the effective-mass approximation to simplify Eq. (6.13) further as

$$(E_{gap} + \frac{Q_i^2}{2M} + \frac{p^2}{2\mu})f_p^{(\nu_i)} - \frac{1}{L} \frac{e^2}{4\pi\epsilon_0} \sum_q U_q f_{p-q}^{(\nu_i)} = E_i f_p^{(\nu_i)}. \quad (6.6)$$

We bring the prefactor  $\frac{e^2}{4\pi\epsilon_0}$  before Coulomb interaction term back. We should notice that the dielectric constant  $\epsilon_r$  is almost 1 in 1D, so we ignore it for the calculation. Also, we ignore the  $E_{gap} + \frac{Q_i^2}{2M}$  for a moment since the total momentum is fixed for given exciton and the gap of band is also fixed. Therefore, we convert 6.6 into

$$\frac{p^2}{2\mu} f_p^{(\nu_i)} - \frac{1}{L} \frac{e^2}{4\pi\epsilon_0} \sum_q U_q f_{p-q}^{(\nu_i)} = E_{\nu_i} f_p^{(\nu_i)}. \quad (6.7)$$

Here we need to be very careful of the dimensionless procedure, we related the Eq. (6.7) with Bohr radius and Rydberg constant as followed

$$\frac{p^2}{2m} \frac{m}{\mu} f_p^{(\nu_i)} - \frac{1}{L} \frac{e^2}{4\pi\epsilon_0} \sum_q U_q f_{p-q}^{(\nu_i)} = E_{\nu_i} f_p^{(\nu_i)}. \quad (6.8)$$

And then we divide the Rydberg constant on both sides, and get

$$\frac{k^2 a_0^2}{2} \frac{m}{\mu} f_p^{(\nu_i)} - \frac{a_0}{L} \sum_q U_q f_{p-q}^{(\nu_i)} = \widetilde{E}_{\nu_i} f_p^{(\nu_i)}. \quad (6.9)$$

Switching from a discrete sum over  $q$  quantized in  $\frac{2\pi}{L}$  into an integral, we get

$$\frac{k^2 a_0^2}{2} \frac{m}{\mu} f_p^{(\nu_i)} - \frac{1}{2\pi} \int dq U_q f_{p-q}^{(\nu_i)} = \widetilde{E}_{\nu_i} f_p^{(\nu_i)}. \quad (6.10)$$

By defining the  $\tilde{k} = ka_0$  and  $\tilde{q} = qa_0$ , we finally get an equation which is completely dimensionless as

$$\frac{\tilde{k}^2}{2} \frac{m}{\mu} f_{\tilde{k}}^{(\nu_i)} - \frac{1}{2\pi} \int_{-\pi \frac{a_0}{L}}^{+\pi \frac{a_0}{L}} d\tilde{q} U_{\tilde{q}} f_{\tilde{k}-\tilde{q}}^{(\nu_i)} = \widetilde{E}_{\nu_i} f_{\tilde{k}}^{(\nu_i)}. \quad (6.11)$$

Fig. 8 shows the eigenenergies of both the standard hydrogen case as  $-\frac{1}{2n^2}$  with bare Coulomb potential and 1D excition case with correct Coulomb matrix element. Different from the 1D hydrogen case, the energy of the 1D excition problem with effective Coulomb potential is different for even and odd states. As we expected, the energy of exciton is higher than the 1D hydrogen case since its potential is shallower, while they converge gradually since its potential converge asymptotically to  $-\frac{1}{\rho}$  near infinity like the 1D hydrogen case.

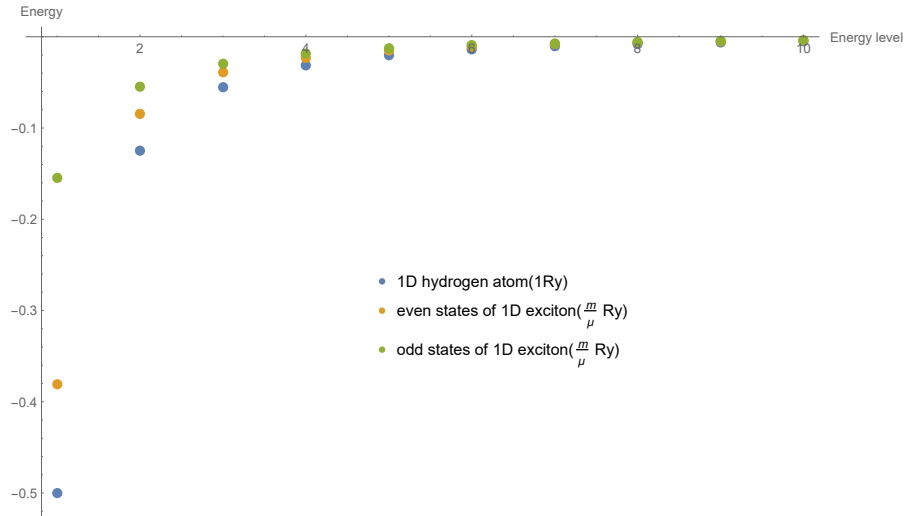


Figure 8: Eigenenergies vs. different energy levels. The energy scale of exciton is  $\frac{m}{\mu}$  Rydberg unit of energy in the figure. The behaviour the 1D hydrogen problem with effective Coulomb potential approaches gradually to the standard 1D hydrogen solution when the energy gets closer to the zero.

We can also compare the wavefunctions of a 1D hydrogen atom and the 1D excition with effective Coulomb potential. As we expected, the wave function of the 1D exciton is less concentrated and spread wider due the less singular potential in the short-distance limit.

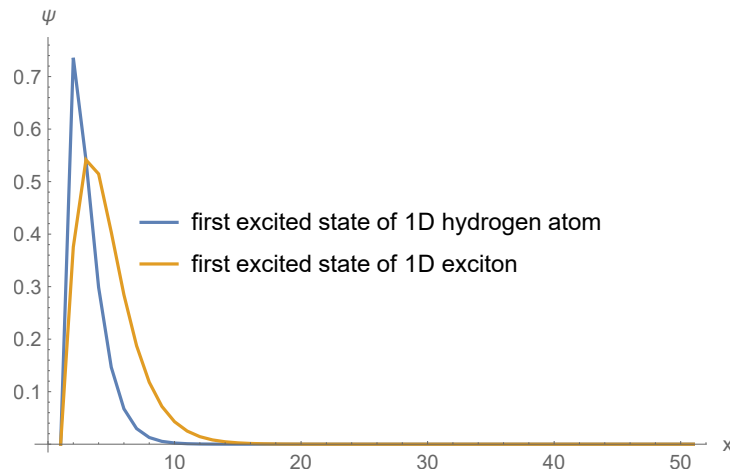


Figure 9: Comparison between wave function of a 1D hydrogen atom and wave function of the 1D exciton.

### 6.3 Numerical solution of the exciton dispersion relation with full band structure

When we consider non zero total momentum  $Q$ , the effective mass approximation is not valid anymore (also not in  $Q=0$ !). Therefore, we need to introduce the full dispersion relation under the electron-hole band structure. We run the numerical calculation within the first Brillouin zone, which means we choose  $-\frac{\pi}{a} < k_e < +\frac{\pi}{a}$ ,  $-\frac{\pi}{a} < k_h < +\frac{\pi}{a}$  and  $-\frac{2\pi}{a} < Q < +\frac{2\pi}{a}$ .

The energy of a free electron-hole pair is defined as minimum under given total momentum  $Q$ . We need to choose a particular  $p$  to get the minimum,

$$\epsilon_{p+\frac{1}{2}Q_i}^{(e)} + \epsilon_{-p+\frac{1}{2}Q_i}^{(h)}. \quad (6.12)$$

It is also important to make the Hamiltonian of the exciton dimensionless. Different from effective-mass approximation, we choose hopping terms  $t$  as energy scale and lattice constant  $a$  as length scale

$$(\epsilon_{\bar{p}+\frac{1}{2}\bar{Q}_i}^{(e)} + \epsilon_{-\bar{p}+\frac{1}{2}\bar{Q}_i}^{(h)})f_{\bar{p}}^{(\nu_i)} - \frac{1}{2\pi} \frac{a_0 E_0}{a t} \int_{-\pi}^{+\pi} d\bar{q} U(\frac{a_0}{a}\bar{q}) f_{\bar{p}-\bar{q}}^{(\nu_i)} = \bar{E}_i f_{\bar{p}}^{(\nu_i)}, \quad (6.13)$$

where  $t$  is the hopping term and  $E_0$  is the Rydberg constant. As we can see from Fig. 10, the energy of the exciton is lower than the free electron-hole pair in the same band structure. This means the exciton state is favored by lowering the energy for the system.

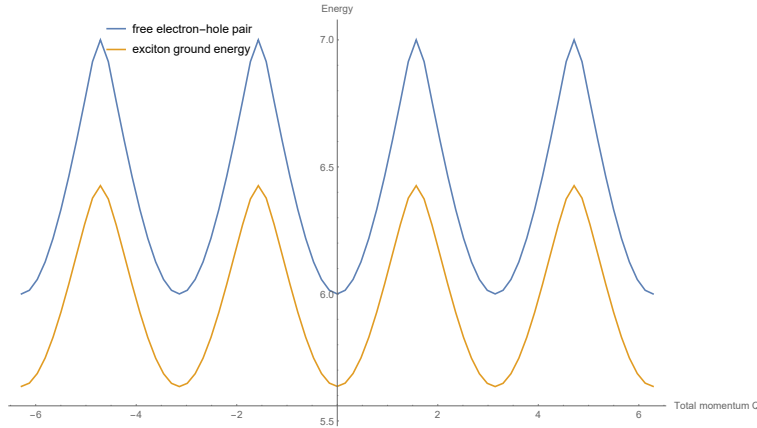


Figure 10: Blue line: Energy of a free electron-hole pair with nonzero total momentum. Orange line: Energy of an exciton with nonzero total momentum. The energy difference between a free pair and an exciton is rescaled by  $(\frac{a}{a_0} \frac{t}{E_0})^2$ .

## 7 Topological properties of excitons

Just like section 2.3, we can calculate the topological invariant of the Wannier exciton by the same procedure. We first write down the formula for the winding number as

$$\gamma = \frac{i}{2\pi} \int_{-2\pi}^{+2\pi} dQ \langle i | \frac{\partial}{\partial Q} | i \rangle, \quad (7.1)$$

$$= \frac{i}{2\pi} \int_{-2\pi}^{+2\pi} dQ \int dx_1 dx_2 \langle i | x_2 x_1 \rangle \frac{\partial}{\partial Q} \langle x_1 x_2 | i \rangle. \quad (7.2)$$

The next step is to write out the expression for  $\langle x_1 x_2 | i \rangle$ . Recall the relation between the exciton creation operator and the electron-hole operator

$$B_i^+ = \sum_p f_p^{(\nu_i)} a_{p+\frac{1}{2}Q_i}^+ b_{-p+\frac{1}{2}Q_i}^+. \quad (7.3)$$

By using the above relation we can write down the exciton wavefunction in real space as

$$\langle x_1, x_2 | i \rangle = \langle x_1, x_2 | B_i^+ | vac \rangle, \quad (7.4)$$

$$= \sum_p f_p^{(\nu_i)} \langle x_1, x_2 | a_{p+\frac{1}{2}Q_i}^+ b_{-p+\frac{1}{2}Q_i}^+ | vac \rangle, \quad (7.5)$$

$$= \sum_p f_p^{(\nu_i)} \langle x_1, x_2 | k_e k_h \rangle. \quad (7.6)$$

where  $k_e = p + \frac{1}{2}Q_i$  and  $k_h = -p + \frac{1}{2}Q_i$ .

The next step is to convert the  $\langle x_1, x_2 | k_e k_h \rangle$  to the Bloch basis  $\langle x_1 | k_e, s \rangle$  and  $\langle x_2 | k_h, p \rangle$ , with the help of the eigenvectors  $|m(k)\rangle$  found in section 2. The basic idea is that we can use the model matrix M to build the bridge between the basis when we diagonalize the hamiltonian.

$$E = M^{-1} H_0(k) M \quad (7.7)$$

where  $M = (|m_1(k)\rangle, |m_2(k)\rangle)$  is formed with the eigenvectors of  $H_0$  as columns in M. For further calculations, we need to write out the matrix form of M as

$$M = \begin{pmatrix} m_{11} & m_{12} \\ m_{21} & m_{22} \end{pmatrix}. \quad (7.8)$$

With the help of the model matrix M, we can write the  $\langle x_1, x_2 | k_e k_h \rangle$  into the original s and p wave basis as

$$\langle x_1, x_2 | k_e k_h \rangle = [m_{12}(k_e) \langle x_1 | k_e, s \rangle + m_{22}(k_e) \langle x_1 | k_e, p \rangle] \otimes [m_{11}^*(-k_h) \langle x_2 | k_h, s \rangle + m_{21}^*(-k_h) \langle x_2 | k_h, p \rangle] \quad (7.9)$$

$$= \frac{1}{L} \left\{ m_{12}(+k_e) m_{11}^*(-k_h) e^{ik_e x_1 + ik_h x_2} + m_{12}(+k_e) m_{21}^*(-k_h) e^{ik_e x_1 + ik_h x_2} \right. \\ \left. + m_{22}(+k_e) m_{11}^*(-k_h) e^{ik_e x_1 + ik_h x_2} + m_{12}(+k_e) m_{22}^*(-k_h) e^{ik_e x_1 + ik_h x_2} \right\}. \quad (7.10)$$

Now we transform momentum  $k_e$  and  $k_h$  into the center-of-mass representation as p and  $Q_i$  by the relation  $k_e = +p + \frac{1}{2}Q_i$  and  $k_h = -p + \frac{1}{2}Q_i$  as

$$\langle x_1 x_2 | k_e k_h \rangle = \begin{pmatrix} m_{12}(p + \frac{1}{2}Q_i) m_{11}^*(+p - \frac{1}{2}Q_i) \\ m_{12}(p + \frac{1}{2}Q_i) m_{21}^*(+p - \frac{1}{2}Q_i) \\ m_{22}(p + \frac{1}{2}Q_i) m_{11}^*(+p + \frac{1}{2}Q_i) \\ m_{22}(p + \frac{1}{2}Q_i) m_{21}^*(+p + \frac{1}{2}Q_i) \end{pmatrix} \cdot \frac{e^{i(p+\frac{1}{2}Q_i)x_1 + i(-p+\frac{1}{2}Q_i)x_2}}{L}. \quad (7.11)$$

Substituting the Eq. (7.11) into Eq. (7.6), we get the expression of the exciton wavefunction in s and p wave basis.

$$\langle x_1 x_2 | i \rangle = \sum_p f_p^{\nu_i} \begin{pmatrix} m_{12}(p + \frac{1}{2}Q_i)m_{11}^*(+p - \frac{1}{2}Q_i) \\ m_{12}(p + \frac{1}{2}Q_i)m_{21}^*(+p - \frac{1}{2}Q_i) \\ m_{22}(p + \frac{1}{2}Q_i)m_{11}^*(+p + \frac{1}{2}Q_i) \\ m_{22}(p + \frac{1}{2}Q_i)m_{21}^*(+p + \frac{1}{2}Q_i) \end{pmatrix} \cdot \frac{e^{i(p+\frac{1}{2}Q_i)x_1+i(-p+\frac{1}{2}Q_i)x_2}}{L}. \quad (7.12)$$

We can use short notation  $\sum_p f_p^{\nu_i} \phi_{orbital} \cdot \phi_{plane\ wave}$  or  $\sum_p f_p^{\nu_i} \phi_{orbital} \cdot \phi_{p\ w}$  to represent Eq. (7.12). Similarly as in the band electron case, we can calculate the winding number by

$$\gamma = \frac{i}{2\pi} \int dQ dx_1 dx_2 \langle i | x_2\ x_1 \rangle \frac{\partial}{\partial Q} \langle x_1\ x_2 | i \rangle, \quad (7.13)$$

$$= \frac{i}{2\pi} \int dQ dx_1 dx_2 \sum_p f_p^{\nu_i*} \phi_{orbital}^* \cdot \phi_{p\ w}^* \frac{\partial}{\partial Q} \left[ \sum_p f_p^{\nu_i} \phi_{orbital} \cdot \phi_{p\ w} \right], \quad (7.14)$$

$$= \frac{i}{2\pi} \frac{1}{L^2} \int dQ dx_1 dx_2 \sum_p f_p^{\nu_i*} \phi_{orbital}^* \cdot \phi_{p\ w}^* \left[ \sum_p \frac{\partial f_p^{\nu_i}}{\partial Q} \phi_{orbital} \cdot \phi_{p\ w} + f_p^{\nu_i} \frac{\partial \phi_{orbital}}{\partial Q} \cdot \phi_{p\ w} + f_p^{\nu_i} \phi_{orbital} \frac{\partial \phi_{p\ w}}{\partial Q} \right], \quad (7.15)$$

$$= \frac{i}{2\pi} \frac{1}{L^2} \int dQ dx_1 dx_2 \sum_p f_p^{\nu_i*} \phi_{orbital}^* \cdot \phi_{p\ w}^* \left[ \sum_p \frac{\partial f_p^{\nu_i}}{\partial Q} \phi_{orbital} \cdot \phi_{p\ w} + f_p^{\nu_i} \frac{\partial \phi_{orbital}}{\partial Q} \cdot \phi_{p\ w} + f_p^{\nu_i} \phi_{orbital} \frac{\partial \phi_{p\ w}}{\partial Q} \right], \quad (7.16)$$

$$= \frac{i}{2\pi} \frac{1}{L^2} \int dQ dx_1 dx_2 \sum_p f_p^{\nu_i*} \phi_{orbital}^* \cdot \phi_{p\ w}^* \left[ \frac{\partial f_p^{\nu_i}}{\partial Q} \phi_{orbital} \cdot \phi_{p\ w} + f_p^{\nu_i} \frac{\partial \phi_{orbital}}{\partial Q} \cdot \phi_{p\ w} + f_p^{\nu_i} \phi_{orbital} \frac{\partial \phi_{p\ w}}{\partial Q} \right], \quad (7.17)$$

$$= \frac{i}{2\pi} \int dQ \sum_p f_p^{\nu_i*} \frac{\partial f_p^{\nu_i}}{\partial Q} + \sum_p |f_p^{\nu_i}|^2 \frac{i}{2\pi} \int dQ \phi_{orbital}^* \frac{\partial}{\partial Q} \phi_{orbital} + \frac{i}{2\pi} \frac{1}{L^2} \int dQ dx_1 dx_2 \left( \frac{ix_1}{2} + \frac{ix_2}{2} \right). \quad (7.18)$$

The first term of Eq. (7.18) is zero because it can be expressed as a total derivative of  $\phi_{orbital}^* \phi_{orbital}$  which is periodic in Q and a real number. The third term is also zero because it is an odd function. As a result, the winding number equals

$$\gamma = \sum_p |f_p^{\nu_i}|^2 \frac{i}{2\pi} \int dQ \phi_{orbital}^* \frac{\partial}{\partial Q} \phi_{orbital}. \quad (7.19)$$

We can calculate the  $\int dQ \phi_{orbital}^* \frac{\partial}{\partial Q} \phi_{orbital}$  by mathematica, which turns out it is insensitive to the relative momentum p. Plus, we know that the eigenstate of the exciton is normalized, which means  $\sum_p |f_p^{\nu_i}|^2 \frac{i}{2\pi} = 1$ . Therefore, the winding number can be simplified further to

$$\gamma = \int dQ \phi_{orbital}^* \frac{\partial}{\partial Q} \phi_{orbital}. \quad (7.20)$$

As an example by setting  $\bar{V} = -2$  and  $\bar{\epsilon} = 1$ , we get  $\gamma = -2$  by Mathematica. This is reasonable because an exciton can be viewed as two copies of band electrons by turning off Coulomb interaction.

## 8 Conclusion

We calculated the dispersion relation of an exciton living in an s-p wave hybrid chain by a tight-binding model, which is beyond the effective mass approximation. The study of the dispersion relation is always essential in solid-state physics. We have also found that the exciton inherits the topology of the electron and the hole. The winding number of an exciton is twice the single-electron winding number, which can be explained by taking a weak limitation towards the zero Coulomb interaction. Such a continuous change should not change any topology.



## References

- [1] Neil W Ashcroft, N David Mermin, et al. Solid state physics, 1976.
- [2] Steven H Simon. *The Oxford solid state basics*. OUP Oxford, 2013.
- [3] K v Klitzing, Gerhard Dorda, and Michael Pepper. New method for high-accuracy determination of the fine-structure constant based on quantized hall resistance. *Physical review letters*, 45(6):494, 1980.
- [4] Lev Davidovich Landau and Evgenii Mikhailovich Lifshitz. *Quantum mechanics: non-relativistic theory*, volume 3. Elsevier, 2013.
- [5] David J Thouless, Mahito Kohmoto, M Peter Nightingale, and Marcel den Nijs. Quantized hall conductance in a two-dimensional periodic potential. *Physical review letters*, 49(6):405, 1982.
- [6] Henrik Bruus and Karsten Flensberg. *Many-body quantum theory in condensed matter physics: an introduction*. OUP Oxford, 2004.
- [7] M Zahid Hasan and Charles L Kane. Colloquium: topological insulators. *Reviews of modern physics*, 82(4):3045, 2010.
- [8] Xiao-Liang Qi and Shou-Cheng Zhang. Topological insulators and superconductors. *Reviews of Modern Physics*, 83(4):1057, 2011.
- [9] B Andrei Bernevig. *Topological insulators and topological superconductors*. Princeton university press, 2013.
- [10] Charles L Kane and Eugene J Mele. Quantum spin hall effect in graphene. *Physical review letters*, 95(22):226801, 2005.
- [11] Holger Bech Nielsen and Masao Ninomiya. The adler-bell-jackiw anomaly and weyl fermions in a crystal. *Physics Letters B*, 130(6):389–396, 1983.
- [12] Yisong Zheng and Tsuneya Ando. Hall conductivity of a two-dimensional graphite system. *Physical Review B*, 65(24):245420, 2002.
- [13] Liang Fu and Charles L Kane. Topological insulators with inversion symmetry. *Physical Review B*, 76(4):045302, 2007.
- [14] Babak Seradjeh, JE Moore, and Marcel Franz. Exciton condensation and charge fractionalization in a topological insulator film. *Physical review letters*, 103(6):066402, 2009.
- [15] Yong P Chen. Topological insulator-based energy efficient devices. In *Micro-and Nanotechnology Sensors, Systems, and Applications IV*, volume 8373, page 83730B. International Society for Optics and Photonics, 2012.
- [16] Hartmut Haug and Stephan W Koch. *Quantum theory of the optical and electronic properties of semiconductors*. World Scientific Publishing Company, 2009.
- [17] Gregory H Wannier. The structure of electronic excitation levels in insulating crystals. *Physical Review*, 52(3):191, 1937.
- [18] G Mahan. Many-particle physics. plenum press. ny (1990). 1932.
- [19] Bill Barnes. Optical properties of solids, 2nd edn, by mark fox: Scope: monograph. level: undergraduate, postgraduate, early career researcher, researcher, 2011.
- [20] Monique Combescot and Shiue-Yuan Shiau. *Excitons and Cooper pairs: two composite bosons in many-body physics*. Oxford University Press, 2015.
- [21] Alexander L Fetter and John Dirk Walecka. *Quantum theory of many-particle systems*. Courier Corporation, 2012.
- [22] John Bardeen, Leon N Cooper, and J Robert Schrieffer. Microscopic theory of superconductivity. *Physical Review*, 106(1):162, 1957.

- [23] Zefang Wang, Daniel A Rhodes, Kenji Watanabe, Takashi Taniguchi, James C Hone, Jie Shan, and Kin Fai Mak. Evidence of high-temperature exciton condensation in two-dimensional atomic double layers. *Nature*, 574(7776):76–80, 2019.
- [24] William Barford. Theory of singlet exciton yield in light-emitting polymers. *Physical Review B*, 70(20):205204, 2004.
- [25] Zhigang Wang, Ningning Hao, Zhen-Guo Fu, and Ping Zhang. Excitonic condensation for the surface states of topological insulator bilayers. *New Journal of Physics*, 14(6):063010, 2012.
- [26] Hongyi Yu, Xiaodong Cui, Xiaodong Xu, and Wang Yao. Valley excitons in two-dimensional semiconductors. *National Science Review*, 2(1):57–70, 2015.
- [27] Henk TC Stoof, Koos B Gubbels, and Dennis BM Dickerscheid. *Ultracold quantum fields*, volume 1. Springer, 2009.
- [28] Zahra Khatibi, Roya Ahemeh, and Mehdi Kargarian. Excitonic insulator phase and condensate dynamics in a topological one-dimensional model. *Physical Review B*, 102(24):245121, 2020.
- [29] Michael Victor Berry. Quantal phase factors accompanying adiabatic changes. *Proceedings of the Royal Society of London. A. Mathematical and Physical Sciences*, 392(1802):45–57, 1984.
- [30] Yakir Aharonov and David Bohm. Significance of electromagnetic potentials in the quantum theory. *Physical Review*, 115(3):485, 1959.
- [31] Di Xiao, Ming-Che Chang, and Qian Niu. Berry phase effects on electronic properties. *Reviews of modern physics*, 82(3):1959, 2010.
- [32] J Zak. Berry’s phase for energy bands in solids. *Physical review letters*, 62(23):2747, 1989.
- [33] János K Asbóth, László Oroszlány, and András Pályi. A short course on topological insulators. *Lecture notes in physics*, 919:166, 2016.
- [34] Valerio Magnasco. *Elementary methods of molecular quantum mechanics*. Elsevier, 2006.
- [35] CC J. Roothaan. A study of two-center integrals useful in calculations on molecular structure. i. *The Journal of Chemical Physics*, 19(12):1445–1458, 1951.